On the prediction of shell vibration and sound radiation by different thin-shell theories when a submerged empty cylindrical shell is driven by an axisymmetric force

Marshall V Hall

Kingsgrove, New South Wales, Australia, marshallhall@optushome.com.au

ABSTRACT

When a cylindrical shell is excited by a steady axisymmetric force, axial and radial vibrations travel in the axial direction and undergo continued reflections at the two ends. The radial vibration radiates sound into the surrounding medium. To calculate the displacement of the radial vibration, four "thin shell theories" were examined: Membrane (M), Donnell-Mushtari (D), Flugge-Byrne-Lur'ye (F), and Epstein-Kennard (E). Of these, E makes the fewest approximations and is the most intricate of the twelve catalogued in Leissa's monograph "Vibration of shells". For a cylindrical shell of radius 3.25 m and wall thickness 40 mm (ratio 1.2%), spectra of radial displacement and far-field radiated sound were computed up to 10 kHz. The differences amongst the four theories are negligible over the whole band. When the wall thickness is increased to 200 mm (ratio 6.2%), the spectra are almost identical for frequencies up to around 2.5 kHz, but gradually diverge at higher frequencies. The results indicate that D and F require the wall thickness to not exceed around 10% of the vibration wavelength, whereas M and E allow that ratio to reach (and perhaps surpass) 30%.

1. INTRODUCTION

As an initial step in predicting the vibration of, and sound radiated by, submersible vehicles, a long thin cylindrical shell with a large radius is used as a model. The shell is sealed at both ends by thin circular disks. When a cylindrical shell is excited by a steady axisymmetric (azimuth-independent) force, axial and radial vibrations travel in the axial direction and undergo continued reflections at the two ends. The radial vibration radiates sound into the surrounding medium. To calculate the amplitude of the radial displacement, four "thin shell theories" were selected from the twelve catalogued by Leissa (1993): Membrane (M), Donnell-Mushtari (D), Flugge-Byrne-Lur'ye (F), and Epstein-Kennard (E). Of these, E makes the fewest approximations and is the most intricate theory of the twelve. The aim of this paper is to examine the differences amongst the results produced by these four theories when applied to a particular shell. It is an extension of Hall (2015a), which presented results for the M theory (although the theory was not there called by that name). A difference between Hall (2015a) and the current approach is that the former included conventional "smearing" corrections (Caresta and Kessissoglou, 2009) for ring stiffeners and added mass attached to the shell. As a result of including those effects it was necessary to confine the calculations to frequencies below around 100 Hz. The neglect of those effects in the present paper allows high frequencies to be examined, where differences amongst the theories become evident.

2. THE CYLINDRICAL SHELL

The three cylindrical coordinates used are the axial distance (x), azimuth (θ) and radial distance (r). The corresponding components of shell displacement are u, v and w, as shown in Figure 1. Shell radius (actually the radial distance to the mid-point between the inner and outer shell surfaces) is denoted by 'a', wall thickness by h, and shell surface slope in the axial direction, $w' \equiv \partial w/\partial x$, by ϕ. The length of the shell will be denoted by L.

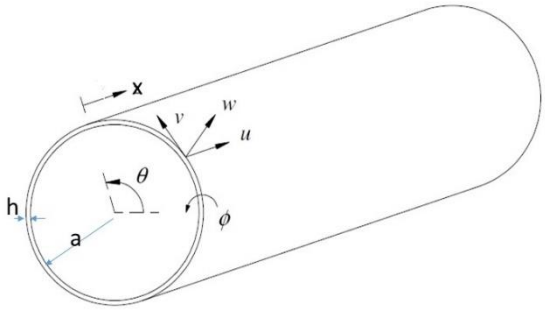

Figure 1: Displacements u=(*u*, *v*, *w*) for a cylindrical shell. Corresponding coordinates are (x, θ, r); x is axial distance, θ is azimuthal angle and r (not shown) is radial distance. Mean shell radius is denoted by 'a', wall thickness by h, and shell surface slope in the axial direction by ϕ.

3. ASSUMPTIONS

In all thin-shell theories, stresses within the shell are assumed to be independent of r; this requires that wall thickness be small (≤ 10%) in relation to shell radius. The normal radial stress σ_r is neglected. Thin-shell theories neglect transverse shear stresses (σ_{xr} , $\sigma_{\theta r}$) as well as $\sigma_{x\theta}$ and rotatory inertia. These are expected to be negligible if $h < \lambda/10$ where λ is the wavelength of the vibration. Thus the only stresses included are the normal axial stress σ_x and normal azimuthal stress σ_θ (the latter is also known as hoop stress σ_H). For the present paper, axial symmetry is assumed. This has three aspects:
(i) there is no azimuthal displacement (twist), $v = 0$,
(ii) the axial and radial displacements are independent of azimuth, $\partial u/\partial\theta = 0, \partial w/\partial\theta = 0$, and
(iii) axial and hoop stresses are independent of azimuth.
The model to be derived here can be applied only if the forcing is axisymmetric.

4. THE MEMBRANE THIN-SHELL THEORY

For M, the simplest theory, the axial Force Resultant (integral of axial stress over *h*) is given by (Leissa 1993: 20) $N_x = \rho_s q_p^2 h(\epsilon_x + \nu\epsilon_\theta)$, where ν, q_p, and ρ_s are the Poisson ratio, plate velocity, and density of the shell material, ϵ is strain. The axial acceleration is obtained from Newton's Law of motion for a continuum: $N_x' = \rho_s h\ddot{u}$, where $\ddot{u}$ is axial acceleration. The resulting axisymmetric equation of axial motion is (Junger & Feit, 1993: 217):

$$u'' + \nu\, w'/a - \ddot{u}/q_p^2 = 0 \tag{1}$$

If the term in w' were absent, Eq. (1) would be a one-dimensional wave equation in terms of *u*. As a result of that term, axial forcing causes the shell to undergo radial motion.

Radial acceleration is obtained by a similar method. This motion may be subject to an external pressure, which will be taken as radiation loading due to induced motion of the exterior medium. The shell interior is assumed here to be a vacuum (the additional term required for a flooded shell is straightforward but omitted). Simplifying the D theory axisymmetric equation of motion for radial acceleration ($\ddot{w}$) presented by Junger & Feit (1993: 217 & 289) to the corresponding equation for M theory yields:

$$\nu\, u'/a + w/a^2 + \ddot{w}/q_p^2 - \dot{w}\, Z/\left(\rho_s q_p^2 h\right) = 0 \tag{2}$$

where Z is the radiation impedance of the external medium to a long cylinder (also known as the Specific Acoustic Impedance). Z is frequency dependent; its low-frequency (LF) and high-frequency (HF) limits are respectively zero and (approximately) the plane-wave impedance of the external medium (product of density and sound-speed). As a result of Z varying with frequency, Eq. (2) can be used only after its Fourier Transform has been taken (since Z is the ratio of two Hankel functions it is unlikely to have an analytical inverse Fourier Transform). Apart from the *h* in the denominator of the expression that corresponds to radiation loading in Eq. (2), M theory is independent of *h*, due to its neglect of any resistance to bending by the shell.

5. THE HIGHER-ORDER THIN-SHELL THEORIES

For all thin-shell theories, the axisymmetric versions of the equations of motion yield a system of two homogeneous partial differential equations (d.e's); one of which contains axial acceleration, as per Eq. (1) for M, and the other contains radial acceleration (and radial velocity due to radiation loading), as per Eq. (2) for M. Each also contains terms in both axial and radial displacements and/or their partial derivatives of various orders up to 4 with respect to axial distance. The extra terms in theories D, F and E, adapted from the catalogue in Leissa (1993: 32-34), are listed in Table 1. The dimensionless thickness parameter β^2 is defined by $\beta^2 = h^2/12a^2$. For clarity, derivatives of orders 3 and 4 are denoted with superscripts of [3] and [4] respectively.

Table 1: Extra terms in the D, F and E equations of motion, relative to the M equations of motion, for axisymmetric cylindrical shells (adapted from Leissa, 1993: 32-34).

	Extra terms in $\ddot{u}$ eqn	Extra terms in $\ddot{w}$ eqn
Donnell-Mushtari (D)	-	$\beta^2\, a^2\, w^{[4]}\, \left(= h^2\, w^{[4]}/12\right)$
Flugge-Byrne-Lur'ye (F)	$-\beta^2\, a\, w^{[3]}$	$\beta^2\, \left(-a\, u^{[3]} +\ w/a^2 + a^2\ w^{[4]}\right)$
Epstein-Kennard (E)	$\beta^2\left(-\nu N_1 u'' + N_4 a^2\, u^{[4]} - N_1\ w'/a - N_2 a\, w^{[3]}\right)$	$\beta^2\left(\nu N_3\, u'/a + 1.5 N_4 a\, u^{[3]} + N_3\ w/a^2 + N_5 w'' + a^2 w^{[4]}\right)$
Coefficients in E terms:	$N_1 = (2 - 9\nu + 6\nu^2)/2(1-\nu)^2$	$N_3 = (1 + 3\nu)/(1-\nu)$
	$N_2 = (2 - 5\nu + \nu^2)/2(1-\nu)^2$	$N_5 = (2 - 2\nu + \nu^2 + 2\nu^3)/2(1-\nu)^2$
	$N_4 = \nu^2/(1-\nu)^2$	

The physical relevance of the extra terms may be described as follows:
D: if the extra term were taken in isolation and added to $\ddot{w}/q_p^2$, the result would be the classical d.e. for transverse displacement (w) of a plate (Leissa 1969: 1). q_p^2 appears because it is proportional to the "flexural rigidity" of the plate. The extra term for D therefore accounts for the normal (radial) stress required to change the shell's radius. D uses the same Force Resultants as M.
F: The extra F terms arise from adding to each Force Resultant a term that includes the rate of change in the axial slope of the shell's middle surface.
E: Theories M, D and F make at least one approximation in most of the many expressions required for the derivation of the equations of motion (Leissa 1993: 7-22). The number of extra terms in Table 1 is small because M, D and F use the same approximations for most of those expressions. E however, does not make any approximation other than those of thin-shell theory, the four postulates of Love (1944: 515-537). It requires more extra terms, and those terms are more intricate.

6. CALCULATION OF PHASE VELOCITIES

In their analysis of axially-dependent vibration of a cylindrical shell using a simplified version of E theory, Junger & Rosato (1954) postulated *u* and *w* to be simple travelling waves, substituted these into the equations of motion, and obtained a linear homogeneous algebraic equation for *u*. They set the coefficient to zero to obtain a "characteristic equation" and explained that the wavenumber roots to that equation for a particular frequency determine the corresponding phase velocities. In contrast, Junger & Feit (1993: 222) assumed that the axial wavenumbers (denoted here by γ) have discrete values and thus used Fourier series to represent the displacements. For each discrete γ they obtained a cubic equation in the square of the "resonance frequency". The method to be used here is similar to that of Junger & Rosato; it assumes γ to be a continuous variable and determines the value(s) it may have for a given frequency. In order to solve the two original partial d.e's, the derivatives with respect to time are first "removed" by taking Frequency-Fourier Transforms of the partial d.e's, yielding two homogeneous ordinary d.e's in $U(x,\omega)$ and $W(x,\omega)$. In this paper, the mathematical Frequency-Fourier Transform is used, for which the

time dependence of the inverse transform is $\exp(+i\omega t)$ (this is opposite to the convention used by Junger & Feit). The derivatives with respect to axial distance are "removed" by taking Wavenumber-Fourier Transforms of the ordinary d.e's, yielding two homogeneous algebraic equations in $\widehat{U}(\gamma,\omega)$ and $\widehat{W}(\gamma,\omega)$. For a given ω, the determinant (Δ) of the four coefficients in these equations is a polynomial in γ^2. For theories M, D, F and E the orders (numbers of roots) are 1, 3, 3 and 4 respectively. Setting Δ = 0 yields the solution for the squared wavenumber, $\gamma_0^2(\omega)$. The significance of obtaining γ_0 is that the Fourier Transform of the axial displacement satisfies the Helmholtz equation:

$$U'' + \gamma_0^2\, U = 0 \tag{3}$$

which has simple solutions $exp(\pm i\gamma_0 x)$, in which the sign depends on the direction of travel (+ for ← and – for →). Since axial phase velocity V is given by:

$$V = \omega/\gamma_0, \tag{4}$$

the analytical result for V obtained by Hall (2015b) using M theory may be expressed as:

$$\gamma_0 = \omega/q_p \;.\; S(q_p)/S(q) \tag{5}$$

where

$$S(q) = \sqrt{q^2/a^2 - \omega^2 + i\omega Z/\rho_s h}\,. \tag{6}$$

in which *i* is the imaginary unit ($+\sqrt{-1}$). Although V depends on frequency, that dependence is not shown explicitly in Eq. (4) or in subsequent expressions (for brevity).

It is straightforward to show that Eq. (5) is equivalent to the result obtained by solving the M theory first-order polynomial for γ^2. It can also be seen from Eqs. (5) and (6) that at LF $(\omega \ll q/a)$, $V \approx q$. At HF $(\omega \gg q/a)$, $V \approx q_p$. As frequency increases from LF to HF, V will transit from q to q_p, and most of the transition will occur at frequencies of the order of $q/2\pi a$ (the shell's ring frequency) where the sum of the first two terms in Eq. (6) is relatively small. The precise frequency at which most transition occurs will depend on the third term in the expression for *S* in Eq. (6), which is inversely proportional to the wall thickness. For theories D, F and E, the first root for which $Real(V) > 0$ and $Imag(V) > 0$ (as produced by the numerical root finder) is provisionally chosen. Since each of the four coefficients in the two algebraic equations can be expressed as the sum of the coefficient for M theory and a term multiplied by β^2, it may be expected that, providing β^2 << 1, $Real(V)$ will lie within a neighbourhood of the (unique) result for theory M. In instances where that is not the case for the first root, the next root is tried.

Since the axial variation of $U(x,\omega)$ is described by $exp(\pm i\gamma_0 x)$ the damping rate in nepers per metre is $|Imag(\gamma_0)|$. This could be converted to nepers per wavelength by multiplying by the wavelength $\lambda = Real(V)/f$ in which *f* is frequency, but it has been found (Hall 2015b) that when $|Imag(\gamma_0)|$ is large this definition may produce two sharp peaks in the damping rate (near both $\omega = q/a$ and $\omega = q_p/a$ for a shell in air). In order to always produce a function with only one peak, the definition has been amended in that $|Imag(\gamma_0)|$ is multiplied by $2\pi/Real(\gamma_0)$ rather than by λ. The difference is negligible if $|Imag(\gamma_0)| \ll Real(\gamma_0)$. The result is then converted to decibels by multiplying by $20/ln(10)$. Damping rate in dB per (quasi) wavelength is therefore defined by

$$DR = 40\pi/ln(10) \;.\; |Imag(\gamma_0)|/Real(\gamma_0)\,. \tag{7}$$

It can be seen from Eq. (5) that at both LF and HF, $Imag(\gamma_0)$ will be approximately proportional to $Imag(q_p)$, the intrinsic loss within the steel, and hence will be small. Apart from intrinsic loss, axial damping corresponds to radiation into the external medium. It can also be seen from Eq. (5) that $Imag(\gamma_0)$ should have a peak frequency of the order of the ring frequency. If h is increased, the peak frequency should approach the ring frequency.

7. SCENARIO

The cylindrical shell to be considered has the same properties as one of the variations of what I call the "University of NSW virtual submersible" without stiffening or added mass (Zhang & Kessissoglou, 2012). The shell is made of steel, with the following properties: Density (ρ) 7800 kg/m^3, Young's Modulus (Y) 210 GPa, Poisson ratio (ν) 0.3, Loss factor: 1/Q = 0.02 (0.55 dB/λ). The corresponding bar velocity (q) is 5190 m/s, and the plate velocity (q_p) is 5440 m/s (to 3 significant figures). The dimensions of the "UNSW" shell are: length (L) 45 m, radius (a) 3.25 m, and thickness (h) 40 mm. For this plate velocity and radius, the ring frequency is 266 Hz. The external medium is water with density (ρ) 1000 kg/m^3 and sound-speed (c) 1500 m/s. The interior is a vacuum.

I also consider an additional shell with a thickness of 200 mm (this shell is approximately neutrally buoyant). Each shell end has a circular disk clamped to it, with the same thickness as the shell.

For the two shell thicknesses, the ratios of thickness to radius are 1.2% & 6.2%. The respective values of β^2 are 1.3×10^{-5} and 3.2×10^{-4}. The estimated maximum frequencies for thin-shell theories to be valid are $f_{max} \sim q_p/(10\,h)$ = 13.6 kHz and 2.6 kHz respectively.

8. RESULTS FOR PHASE VELOCITIES

8.1 Wall thickness 40 mm

For this thickness, thin-shell theories are expected to be valid for frequencies up to around 13 kHz. Results for the phase velocity up to 10 kHz have been calculated for the 40-mm wall for each theory. The curves for the four theories (not shown) overlie each other, except that the Phase Velocity for theory E falls below the others as frequency exceeds around 8 kHz. As expected, the LF limit is the bar velocity and, except for E, the HF limit is the plate velocity. The curves cross the mid-point between the two limits (5315 m/s) at 90 Hz.

Results for the damping rate up to 10 kHz have been calculated for the 40-mm wall for each theory. The curves for the four theories (not shown) overlie each other over the whole band. They exhibit a maximum of 2.6 dB per wavelength at a peak frequency of 85 Hz, and their LF and HF limits are all 0.55 dB/λ (which corresponds to the intrinsic loss factor assumed for the steel).

8.2 Wall thickness 200 mm

Results for the phase velocity up to 10 kHz for the 200-mm wall are shown in Figure 2. Thin-shell theories are expected to be valid for frequencies up to nearly 3 kHz. The curves for the four theories overlie each other, except that the Phase Velocity for theory E begins to fall significantly below the others as frequency exceeds around 1 kHz. Again, the LF limit is the bar velocity and, except for E, the HF limit is the plate velocity. The curves cross the mid-point between the two limits (5315 m/s) at 225 Hz. This "transition frequency" being closer to the ring frequency (266 Hz) than occurred for the 40-mm wall thickness is attributed to the effect of the (five-fold) increase in wall thickness on the third term in Eq. (6).

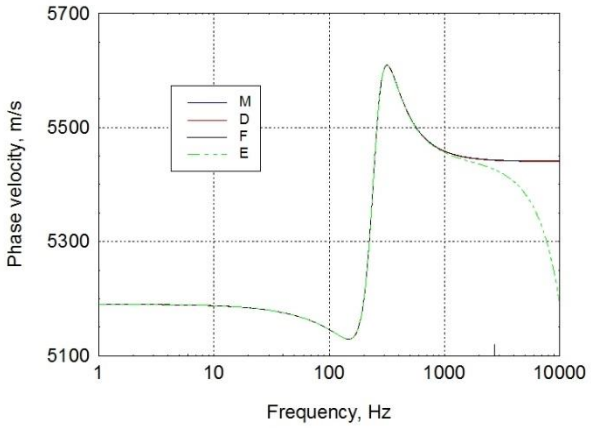

Figure 2: Phase velocities as functions of frequency for the shell with wall thickness 200 mm, for each of the four theories. The vertical line on the abscissa is the estimated maximum frequency for thin-shell theories to be valid.

Results for damping rate up to 10 kHz for the 200-mm wall are shown in Figure 3. The curves for the four theories overlie each other over the whole band. They exhibit a maximum of 5.0 dB per wavelength at a peak frequency of 238 Hz, and their LF and HF limits are again all 0.55 dB/λ. This peak frequency being closer to the ring frequency than occurred for the 40-mm wall thickness is again attributed to the effect of the (five-fold) increase in wall thickness on the third term in Eq. (6).

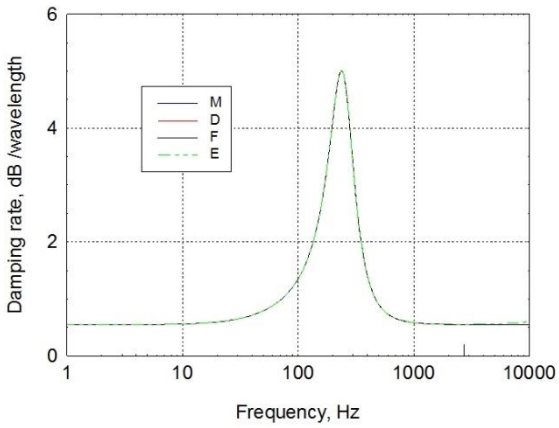

Figure 3: Damping rates as functions of frequency for the shell with wall thickness 200 mm, for each of the four theories.

9. CALCULATION OF RADIAL VIBRATION

A circular disk (with the same thickness as the shell) is clamped to each end of the cylindrical shell. The reflectivity of an axial wave in a cylindrical shell incident on an end disk was computed as described in Hall (2015a). In the cylindrical shell, axial displacement $U(x,\omega)$ due to an axisymmetric force at the stern ($x = 0$) is given by an infinite geometric series in which the first term is

$$U(0,\omega)[exp(-i\,\omega x/V) + R_b\, exp(i\,\omega(x-2L)/V)] \tag{8}$$

where R_b is the reflectivity of the bow. The series ratio is $R_b R_s \exp(-2\,i\,\omega\,T)$, where R_s is the stern reflectivity, and $T = L/V$ is the (complex) stern-to-bow travel time. Since the disks at the two ends are identical it follows that $R_s = R_b$.

Since the shell vibration is driven by a force, we need to express the induced strain in terms of that force. For a solid rod or bar, the axial strain at $x = 0$ would be related to the force by:

$$\vec{U}'(0,\omega) = -F(\omega)/AY \tag{9}$$

where $F(\omega)$ is the harmonic $\left(e^{i\omega t}\right)$ axisymmetric force, A is the cross-sectional area to which F is applied (the cross-sectional area of the rod), and Y is the Young Modulus of the rod material ($\rho_s q^2$). For a shell however, Eq. (9) is inapplicable, notwithstanding that it was used by Hall (2015b). The appropriate expression for a shell is obtained by first taking the Fourier Transform of the conventional expression for axial stress $\sigma_x(x,t)$ in a thin shell (Leissa 1993: 14):

$$\Sigma_x(x,\omega) = [U'(x,\omega) + W(x,\omega)/a]\,Y/(1-\upsilon^2)\,. \tag{10}$$

In the M theory (but not necessarily in the others) the radial displacement W is proportional to the axial strain (Hall, 2015b), and substitution of that relation into Eq. (10) yields

$$\Sigma_x(x,\omega) = \rho_s\, V^2\, U'(x,\omega)\,. \tag{11}$$

Although the applicability of Eq. (11) to theories D, F or E has not been determined, it will be assumed here as an approximation. The strain at x = 0 will therefore be given by

$$\vec{U}'(0,\omega) = -F(\omega)/[A\,\rho_s\,V^2]\,. \tag{12}$$

Since

$$\vec{U}(x,\omega) = U(0,\omega)\,exp(-i\,\omega x/V),$$

the $U(0,\omega)$ required in Eq. (8) is given by

$$U(0,\omega) = \vec{U}'(0,\omega)\;V/(-i\omega) \tag{13}$$

As a result of the algebraic equations (that produced γ_0) being homogeneous, the unknowns $\widehat{U}(\gamma,\omega)$ and $\widehat{W}(\gamma,\omega)$ are zero except at $\gamma = \gamma_0$. Their properties as functions of γ are similar to that of the Dirac delta function $\delta(\gamma-\gamma_0)$. As a result, their inverse Fourier Transforms, $W(x,\omega)$ and $U(x,\omega)$ each contain a factor of $exp(-i\gamma_0 x)$, and their relation is therefore:

$$W(x,\omega) = U(x,\omega)\;\widehat{W}(\gamma_0,\omega)/\widehat{U}(\gamma_0,\omega) \tag{14}$$

The ratio $\widehat{W}/\widehat{U}$ is obtained from either of the two algebraic equations in $\widehat{U}(\gamma,\omega)$ and $\widehat{W}(\gamma,\omega)$, evaluated at $\gamma = \gamma_0$.

The reflectivity R_b of each end is obtained by solving the equation of motion for a flexible circular disk with boundary conditions obtained by matching its displacement, slope and stress to those at the end of the shell (Hall, 2015a). In solving this equation, radiation loading by water on the disks has been neglected, on the basis that a model for the radiation impedance to a flexible disk has not been found. Inertial loading (as distinct from radiation loading) due to an incompressible medium will reduce the resonance frequencies. According to the expression obtained by Lamb (1920) as cited by Leissa (1969: 299) for clamped disks, the fundamental resonance frequencies of the present 40 and 200-mm disks, in contact with water on one side, will be reduced by around 64% and 35% respectively.

Spectra of radial displacement (at a distance of 9.3 m from the stern) for the 40-mm wall and disks have been computed for each of the four thin-shell theories. The four curves (not shown) overlie each other. The first six flexural harmonics (fundamental frequency and the first five overtones) of this disk are 10, 38, 84, 150, 234 and 337 Hz. Peaks at each of these frequencies (to within 1%) are evident in the spectra. In addition to the disk resonances, the shell should exhibit axial resonances when the ratio of the infinite geometric series, $R_b^2\exp(-2\,i\,\omega\;L/V)$ is approximately unity. For this analysis the end reflectivity is set to unity; this should generally cause only a small error since it is at the disk resonances that the reflectivity differs significantly from unity. Because V varies with frequency, the ratios of these frequencies to the fundamental are not integers and identifying them requires a numerical or graphical procedure. The result of this analysis is that the first six axial harmonics are at 58, 119, 181, 242, 303, and 364 Hz. Peaks at five of these six frequencies (to within 3%) are evident in the spectra, the exception being 303 Hz.

Spectra of radial displacement (at a distance of 9.3 m from the stern) for the 200-mm wall and disks are shown in Figure 4. The curves for the four theories overlie each other up to around 2.5 kHz but diverge monotonically at higher frequencies. The M and E curves remain together (even though the E Phase velocity decreased substantially near 10 kHz). The F curve diverges the most and exceeds the M and E curves by 13 dB at 10 kHz. Although the frequency where divergence commences is close to the estimated maximum frequency for any thin-shell theory, it is unclear why there should be a connection between these frequencies.

For this 200-mm disk the first four flexural harmonics are 48, 188, 422, and 749 Hz. The peaks in the radial displacement spectra closest to these harmonics are 45, 196, 445, and 763 Hz. The differences between the disk harmonics and the spectrum peaks are significant, and larger than occurred with the 40-mm disk. The first six axial harmonics are at 58, 114, 171, 240, 312, and 372 Hz. The differences between these harmonics and those for the

thin wall may be attributed to the variation of Phase Velocity with wall thickness, as per Eqs. (4) – (6). There are four peaks in the radial displacement spectra close to these axial harmonics: 60, 110, 161, and 250 Hz (a broad peak).

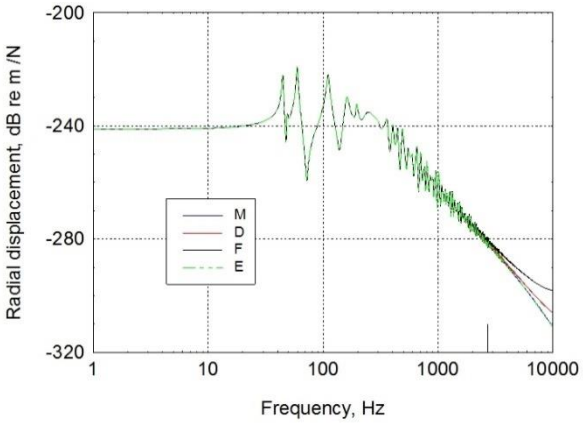

Figure 4: Radial displacement spectra for the 45-m long shell with wall thickness 200 mm, for each of the four theories. Distance from stern is 9.3 m. The vertical line on the abscissa marks the estimated maximum frequency for thin-shell theories.

10. CALCULATION OF FAR-FIELD RADIATED SOUND

The "Transform Formulation of the Pressure Field of Cylindrical Radiators" (Junger & Feit, 1993:173-176) consists of both general and long-range models. The simpler long-range model, the "Stationary-Phase Approximation to the Far-Field of Cylindrical Radiators" is applicable providing the range is so large that:
(1) the Hankel function of range may be replaced by its asymptotic expression over the whole frequency band that affects the result, and
(2) the integral over wavenumber that is contained in the general model may be approximated using the method of stationary phase.
Satisfying condition (2) is not as straightforward as (1). Consider the cylindrical coordinate system used in Figure 1 except that, since the scenario is axisymmetric, azimuth angle is omitted. Consider the cylinder's stern to be located at the origin (0, 0). For simplicity, a hydrophone will be located in the (orthogonal) plane of the bow ($x = L$) at an arbitrary range $r \gg a$. In travelling from the stern to the hydrophone, rays will travel along the cylinder for a distance (χ) from where they will travel through the water to the hydrophone. The loudest waterborne rays are those that make an angle given by $\varphi = \sin^{-1}(c/V)$ with the range axis; Reinhall & Dahl (2011) called these arrivals "Mach waves". Thus the ray that left the cylinder at $\chi = L - r\ \tan\varphi$ will be the loudest at the hydrophone. If we define an "offset" by

$$\delta \equiv r \tan[\sin^{-1}(c/V)] \tag{15}$$

we can say that if $\delta > L$ then the ray will not travel along the cylinder at all but will travel in a straight line from the stern to the hydrophone. The phase of a harmonic sound signal (relative to its phase at the stern) will therefore be given by:

$$\psi(L,r) = -i\omega\,(L-\delta)/V - i\omega\sqrt{r^2+\delta^2}/c \ \text{, if } 0 < \delta \le L, \tag{16}$$

or:

$$\psi(L,r) = -i\omega\sqrt{r^2+L^2}/c \ \text{, if } \delta > L \tag{17}$$

The stationary phase method will be accurate providing the source of the loudest sound is at the stern rather than elsewhere on the cylinder, thus requiring that $\delta > L$. We consider a minimum value of δ, which will correspond to a maximum value of V, for which according to Figure 2 we can set a value of 5600 m/s. For a

hydrophone in the plane of the bow the maximum offset is 45 m (L), for which Eq. (15) gives an orthogonal (perpendicular to the cylinder axis) range of 162 m. This means that a Mach wave from a cylinder 45 m long cannot reach a hydrophone in the plane of the bow if the orthogonal range exceeds around 162 m. As a consequence, the stationary phase method is expected to be a good approximation at ranges well in excess of 162 m. Using the stationary phase method, the resulting expression for the harmonic sound pressure is more conveniently presented in spherical coordinates:

$$R = \sqrt{r^2 + x^2} \qquad \text{and} \qquad \psi = \tan^{-1}(r/x)$$

where R is slant range and ψ is colatitude (angle from the cylinder axis, from the stern). The result given by Junger & Feit (1993:176), but adapted to a time dependence of $\exp(+i\omega t)$, is:

$$P(R,\psi,\omega) = -i\omega^2 \rho e^{-ikR}\, \widehat{W}(k\cos\psi,\omega) \Big/ \Big[\pi R\, k \sin\psi\, H_1^{(2)}(ka\sin\psi)\Big] \tag{18}$$

where $H_1^{(2)}$ is the Hankel function of the second kind and order 1 $\left[H_1^{(2)}(\varsigma) = -d/d\varsigma\ H_0^{(2)}(\varsigma)\right]$, and

$$\widehat{W}(k\cos\psi,\omega) = \int_0^L W(x,\omega)\, exp(-ikx\cos\psi)\, dx \tag{19}$$

in which $W(x,\omega)$ is given by Eq. (14).

The spectra obtained for the four theories using Eq. (18) and the 200-mm wall are shown in Figure 5. The four curves are indistinguishable up to around 2.5 kHz but diverge monotonically at higher frequencies. The M and E curves decrease steadily with increasing frequency and diverge by 1.1 dB at 10 kHz. The D curve diverges by a greater amount and exceeds M at 10 kHz by 5.1 dB. The F curve however passes through a minimum near 7 kHz and then starts to increase so that at 10 kHz it is 13 dB above the M curve. At HF the sound pressure spectra do not fall off as quickly as the vibration spectra, owing to the frequency factors in Eq. (18). The turn-around in the F curve is clearly an anomaly, caused by a slow drop-off in the radial displacement spectra (Figure 4). The peaks in the acoustic spectra are at the same frequencies as the peaks in the radial displacement spectra, and hence correspond to the resonances identified in Section 9.

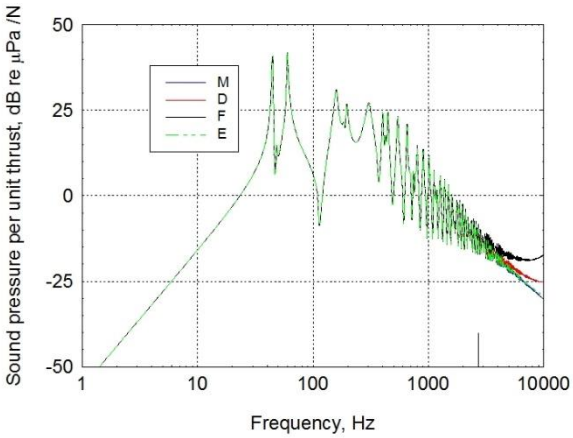

Figure 5: Spectra of radiated sound at range 1000 m and in the plane of the bow of the cylindrical shell with wall thickness 200 mm, for each of the four theories. The vertical line on the abscissa marks the estimated maximum frequency for thin-shell theories.

11. SUMMARY AND CONCLUSIONS

To calculate the displacement of the radial vibration generated in a cylindrical shell excited by a steady axisymmetric force, four "thin shell theories" have been examined: Membrane (M), Donnell-Mushtari (D), Flugge-Byrne-Lur'ye (F), and Epstein-Kennard (E).

For a cylindrical shell of radius 3.25 m and wall thickness 40 mm (ratio 1.2%), the spectra of the radial displacement and the far-field radiated sound were computed up to 10 kHz. The differences amongst the four theories are negligible over the whole band.

When the wall thickness is increased to 200 mm (ratio 6.2%), the differences amongst the spectra are negligible for frequencies up to around 2.5 kHz. At higher frequencies, the four spectra of both parameters gradually diverge. For displacement at 10 kHz, M and E predict the least vibration, and D and F exceed them by 5 and 13 dB respectively. For sound radiation at 10 kHz, M yields the lowest level, and D, F and E exceed M by 5, 13, and 1 dB respectively.

Although the four theories were not designed to be applied to thick shells, M and E theories produce apparently accurate vibration spectra to the maximum frequency examined, where the wall thickness is around 30% of the vibration wavelength. D and F require the wall thickness to not exceed around 10% of the vibration wavelength, whereas M and E allow that ratio to reach (and perhaps surpass) 30% (calculations at higher frequencies were tried but failed due to numerical problems). The errors in D and F at higher frequencies are attributable to the presence of fourth and third order derivatives respectively, which grow rapidly as frequency increases. These derivatives also occur in E theory, but presumably with smaller coefficients.

ACKNOWLEDGEMENTS

Two anonymous reviewers made useful comments on the first draft.

REFERENCES

Caresta, M & Kessissoglou, NJ 2009, 'Structural and acoustic responses of a fluid-loaded cylindrical hull with structural discontinuities', *Applied Acoustics*, vol. 70, pp. 954 – 963.

Hall, MV 2015a, 'An analytical model for noise radiated from axial vibration of a simplified pressure hull of an underwater vehicle', *Proceedings of Acoustics 2015 - Hunter Valley, Annual Conference of the Australian Acoustical Society*, NSW Division Australian Acoustical Society

Hall, MV 2015b, 'An analytical model for the underwater sound pressure waveforms radiated when an offshore pile is driven', *Journal of the Acoustical Society of America,* vol. 138, pp. 795 – 806.

Junger, MC & Feit, D 1993, *Sound, Structures, and Their Interaction*, Acoustical Society of America, New York.

Junger, MC & Rosato, FJ 1954, 'The propagation of elastic waves in thin-walled cylindrical shells', *Journal of the Acoustical Society of America,* vol. 26, pp. 709 – 713.

Lamb, H 1920, 'On the vibrations of an elastic plate in contact with water', *Proceedings of the Royal Society of London, Series A*, vol. 98, pp. 205-216.

Leissa, AW 1969, *Vibration of Plates*, National Aeronautics and Space Administration, Washington, D.C.

Leissa, AW 1993, *Vibration of Shells*, American Institute of Physics, Woodbury, New York.

Love, AEH 1944, *A Treatise on the Mathematical Theory of Elasticity,* 4th edn, Dover Publications, New York.

Reinhall, PG and Dahl, PH 2011, 'Underwater Mach wave radiation from impact pile driving: Theory and observation,' *Journal of the Acoustical Society of America*, vol. 130, pp. 1209–1216.

Zhang, C & Kessissoglou, NJ 2012, 'Effect of excitation loads on the low frequency structural responses of a submerged hull', *Proceedings of Acoustics 2012 - Fremantle, Annual Conference Of The Australian Acoustical Society*, WA Division Australian Acoustical Society.